Electronic Supplementary Material (ESI) for ChemComm.

Supporting Information

Chain-capper effect to bias the amplification of asymmetry in supramolecular polymers

Cristina Naranjo,[a] Yeray Dorca,[a] Goutam Ghosh,[b] Rafael Gómez,[a] Gustavo Fernández,*[b] Luis Sánchez[a]*

[a]*Departamento de Química Orgánica, Facultad de Ciencias Químicas, Universidad Complutense de Madrid, E-28040 Madrid (Spain).*
[b]*Organisch-Chemisches Institut, Westfälische Wilhelms-Universität Münster, Corrensstraße 36, 48149 Münster (Germany)*

Contents:

1. Supplementary Figures and Tables

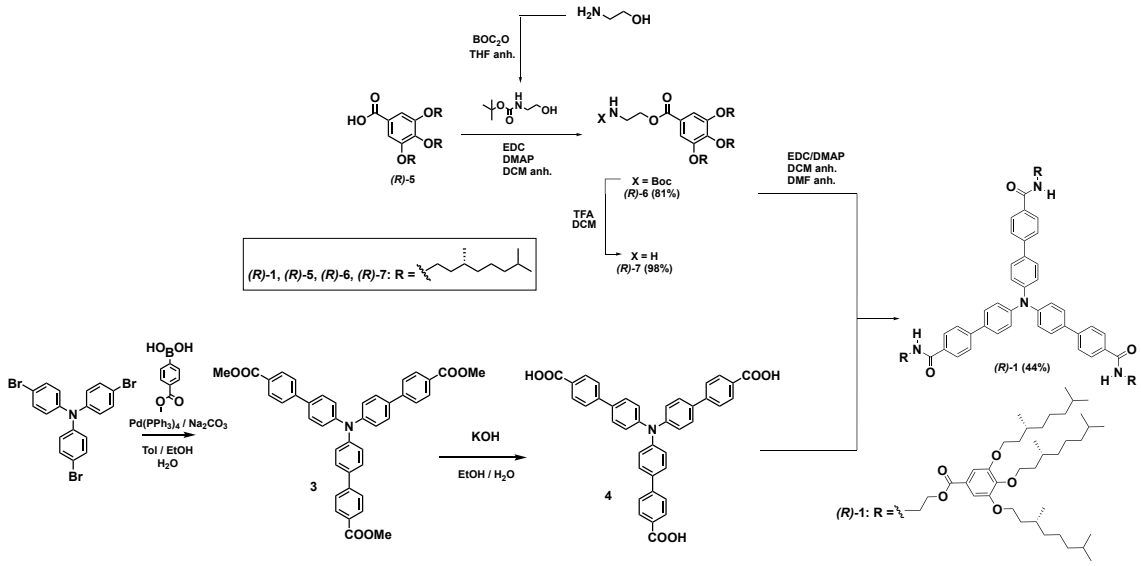

Scheme S1. Synthetic route for trisbiphenylamine-tricarboxamides ***(S)-1*** and ***(R)-1.***

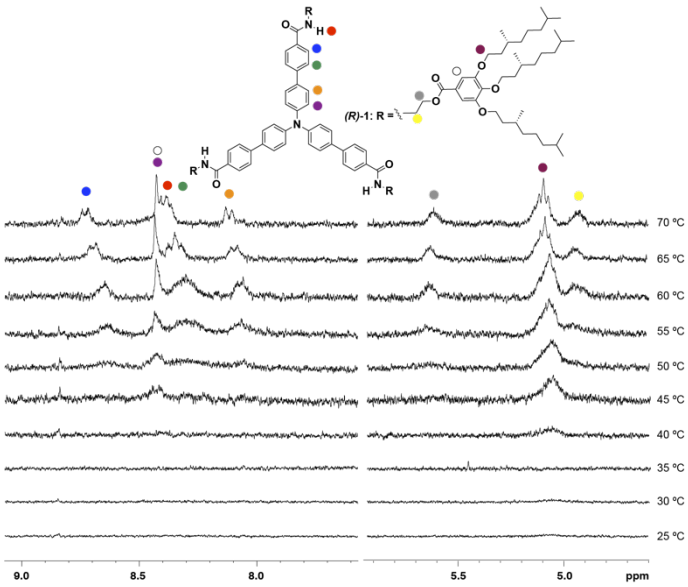

Figure S1. Partial ^{1}H NMR spectra of ***(R)*-1** in MCH-d_{14} at different temperatures showing the aromatic, the amide and some of the aliphatic protons (c_T = 1 mM).

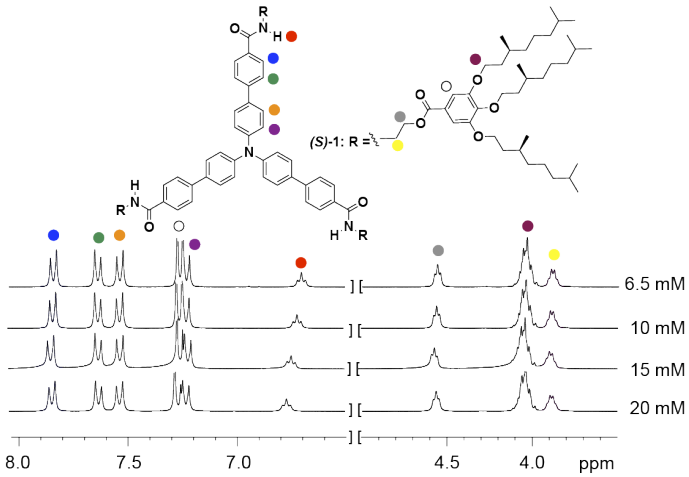

Figure S2. Partial ^{1}H NMR spectra of ***(S)*-1** in $CDCl_3$ at different concentrations showing the aromatic, the amide and some of the aliphatic protons (298 K).

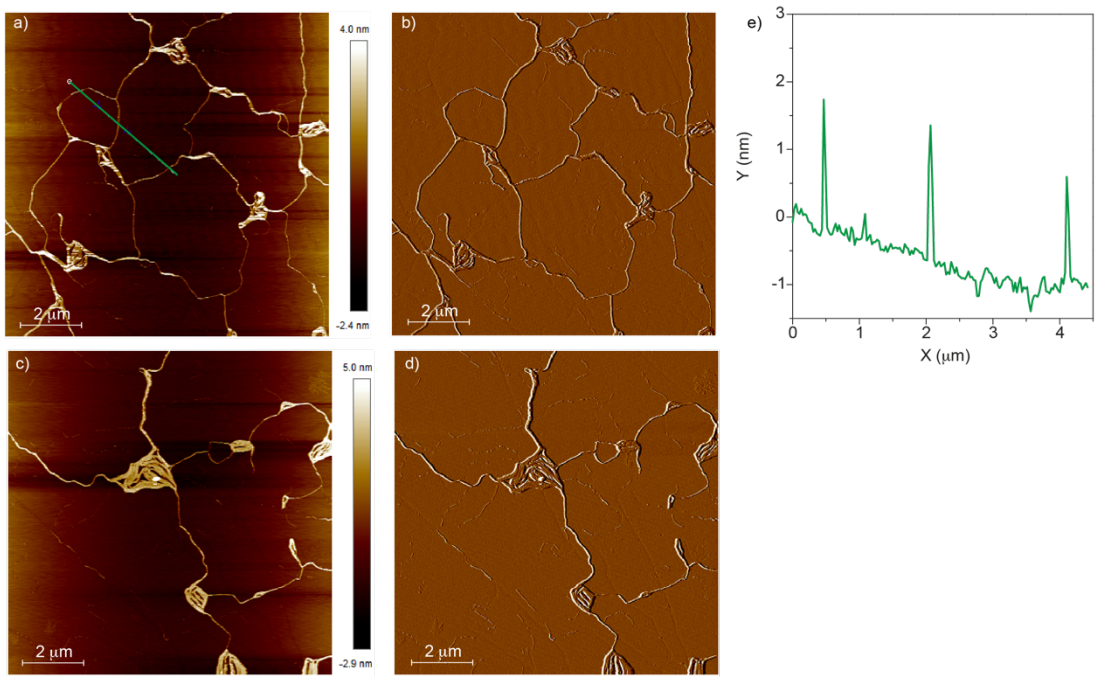

Figure S3. (a,c) Height and (b,d) phase AFM images of the fibrillar supramolecular polymers formed from ***(S)*-1** in MCH spin-coated onto mica (298 K; c_T = 10 µM); e) Profile of the aggregates of ***(S)*-1** along the green line in (a).

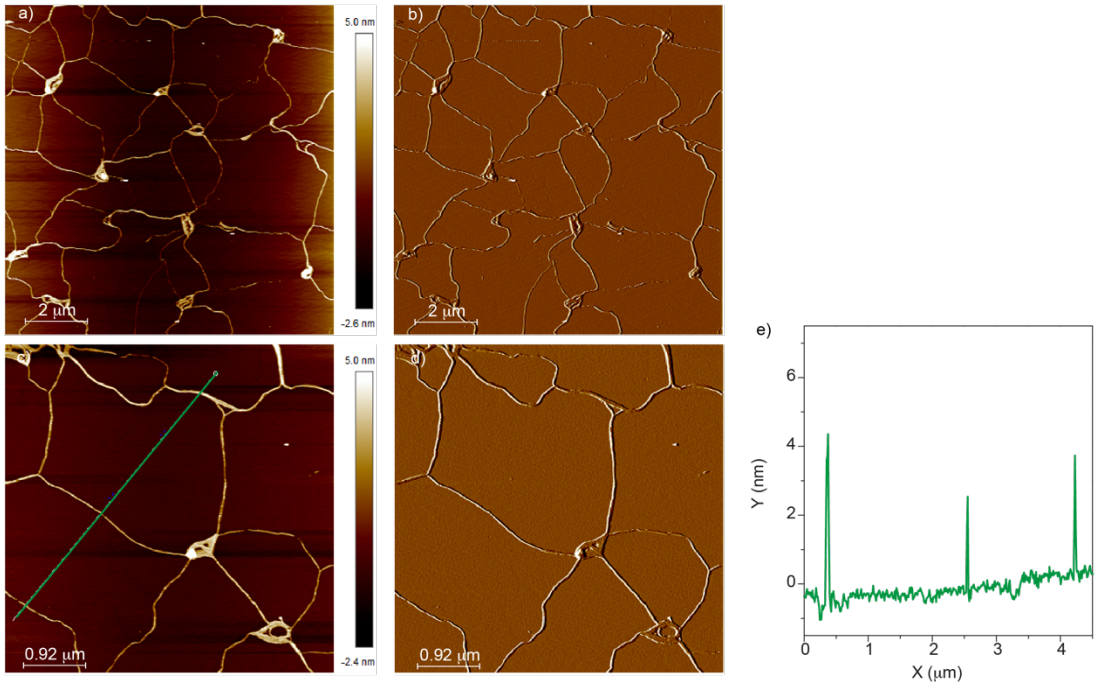

Figure S4. (a,c) Height and (b,d) phase AFM images of the fibrillar supramolecular polymers formed from ***(R)*-1** in MCH spin-coated onto mica (298 K; c_T = 10 µM); e) Profile of the aggregates of ***(R)*-1** along the green line in (a).

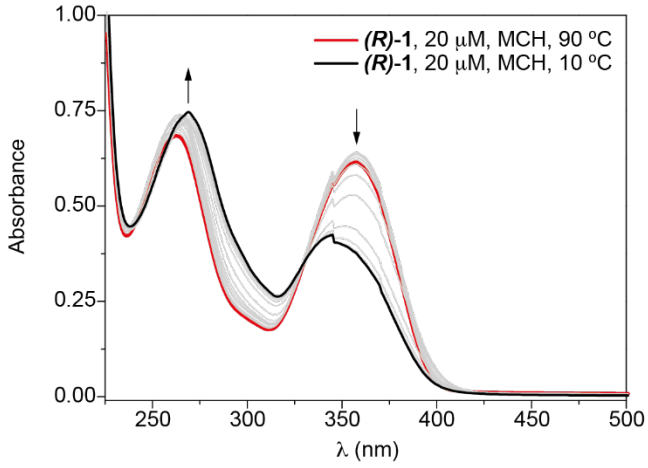

Figure S5. UV-Vis spectra of **(*R*)-1** in MCH at c_T = 20 µM. Arrows indicate the absorption changes upon decreasing temperature.

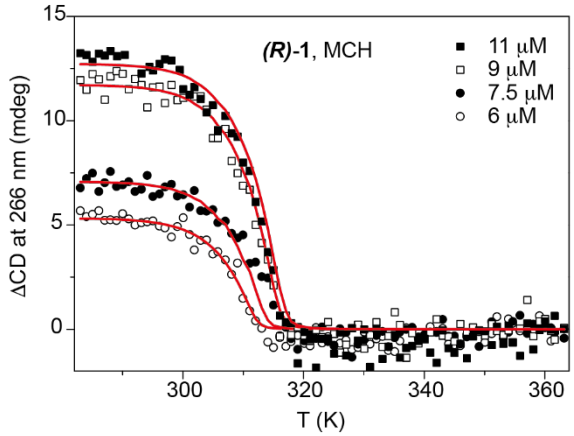

Figure S6. Plot of the variation of the dichroic signal of ***(R)*-1** at λ = 266 nm versus temperature, cooling at 1 K min^{-1}. Red curves correspond to the fit to the EQ model.

Table S1. Thermodynamic parameters derived for ***(S)*-1** and ***(R)*-1** in MCH by applying the one-component EQ model.

	ΔH_e[a]	ΔS[b]	ΔH_n[a]	σ (–)	K_e[c]	K_n[c]	ΔH_{mm}[a]
***(S)*-1**	-152.8±8	-425±27	-27.3±2	3.9×10^{-3}	5.3×10^{6}	2.1×10^{3}	–1.2±0.05
***(R)*-1**	-150.5±9	-383±30	-15.5±2	1.8×10^{-3}	2.4×10^{6}	4.5×10^{3}	

[a] In kJ/mol; [b] in JK/mol; [c] in L/mol; [d] The equilibrium constants for elongation and dimerization, K_e and K_n, and the cooperativity factor σ (= K_n / K_e) are calculated at 298 K.

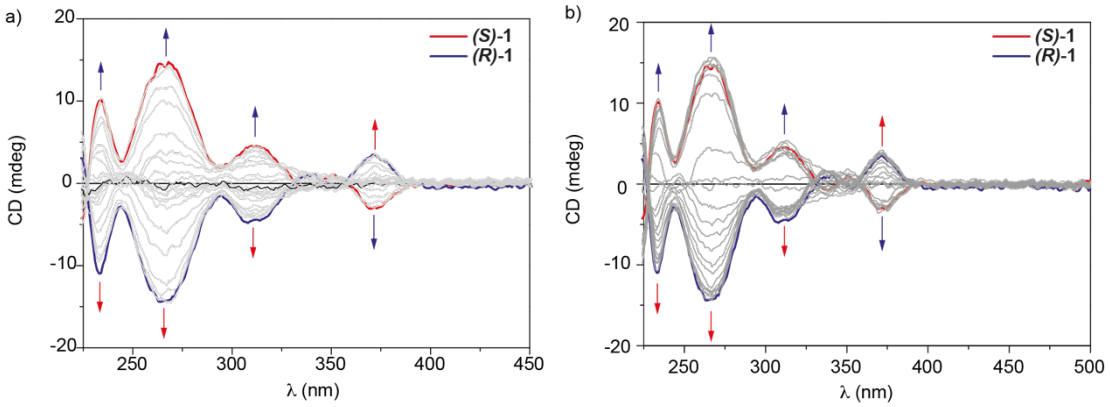

Figure S7. CD spectra for mixtures of ***(S)*-1** and ***(R)*-1** recorded upon heating the mixture at 90 ºC, cooling it down to 20 º C and after a stabilization time of 10 min (a) and after aging the mixture for 24 h (b). Experimental conditions: MCH, c_T = 20 μM. Blue and red arrows indicate the changes upon increasing *ee* of tricarboxamides ***(S)*-1** and ***(R)*-1**, respectively.

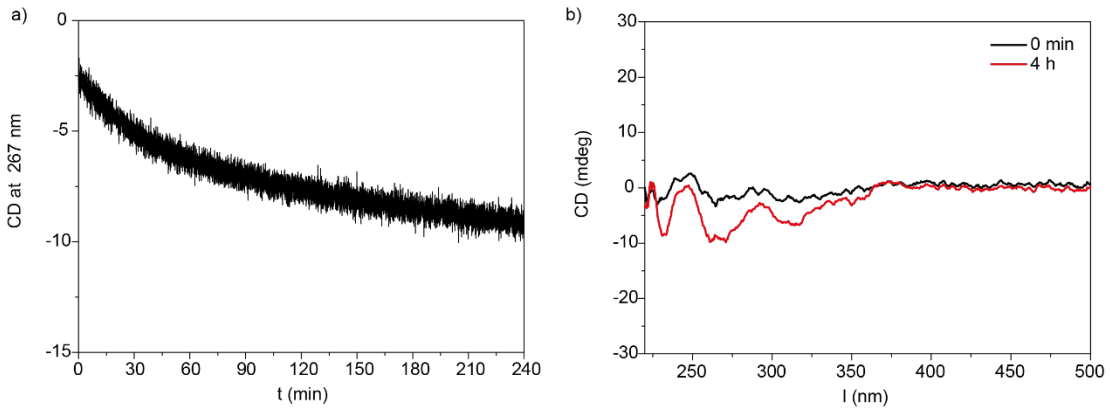

Figure S8. (a) Time profile of the evolution of the dichroic response of a mixture of ***(S)*-1** and ***(R)*-1**; (b) CD spectra of the mixture ***(S)*-1** and ***(R)*-1** at *ee*= 0.4 and c_T = 20 μM at t = 0 and t = 4 h. Experimental conditions: MCH, *ee*= 0.4, c_T = 20 μM, 298 K.

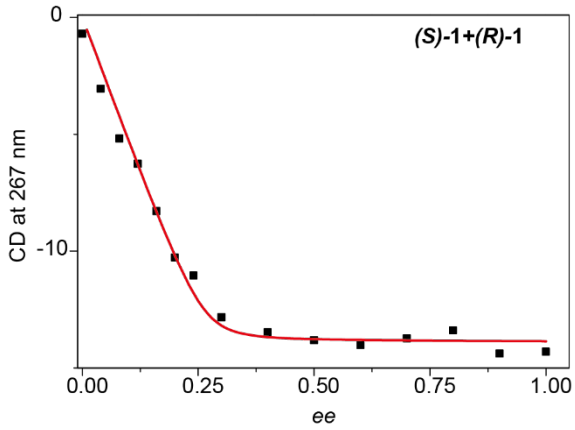

Figure S9. Changes in CD intensity at λ = 267 nm as a function of *ee* upon adding ***(S)*-1** to a solution of ***(R)*-1** (MCH, c_T = 20 μM) at 20 ºC. *ee* = 1.0 corresponds to pure ***(S)*-1**. The red line depicts the fitting to the two-components EQ model.

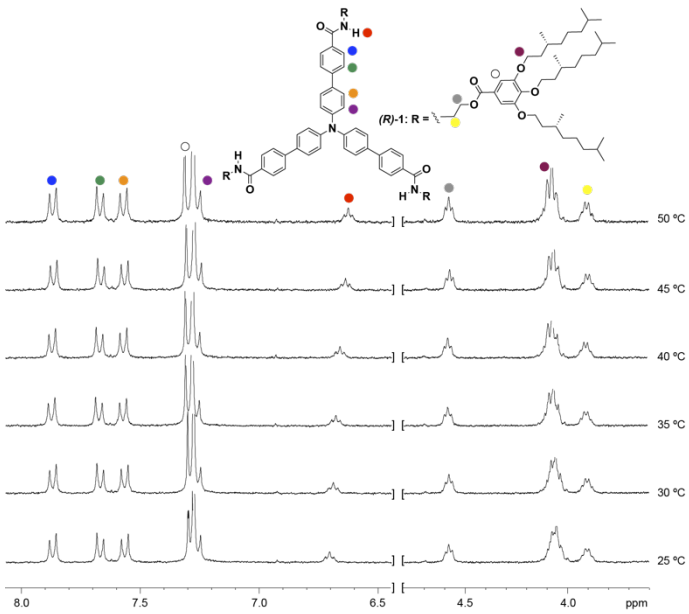

Figure S10. Partial ^{1}H NMR spectra of ***(R)*-1** in $CDCl_3$ at different temperature showing the aromatic, the amide and some of the aliphatic protons (c_T = 1mM).

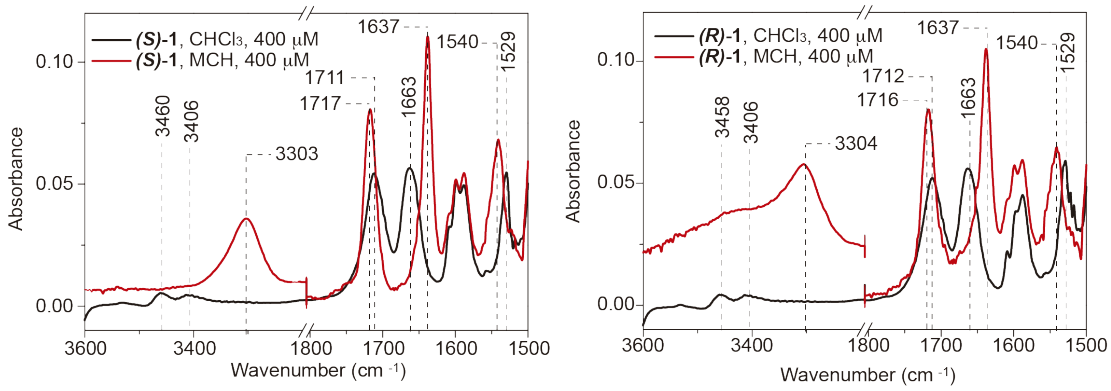

Figure S11. Partial FTIR spectra of ***(S)*-1** and ***(R)*-1** in MCH (red) and $CHCl_3$ (black) showing the region in which the stretching N-H and Amide I bands appear (c_T = 400 μM; 298 K).

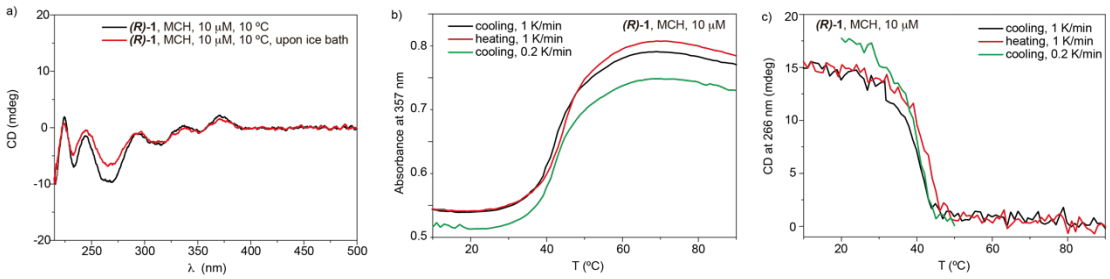

Figure S12. a) CD spectra of ***(R)*-1** at 10 °C after cooling a solution at 1 K/min and upon quenching into an ice bath; b) cooling (black and green) and heating (red) curves obtained by plotting the variation of the absorbance at 357 nm by using rates of 1 K/min (black and red curves) and 0.2 K/min (green curve); c) cooling (black and green) and heating (red) curves obtained by plotting the variation of the dichroic response at 266 nm by using rates of 1 K/min (black and red curves) and 0.2 K/min (green curve).

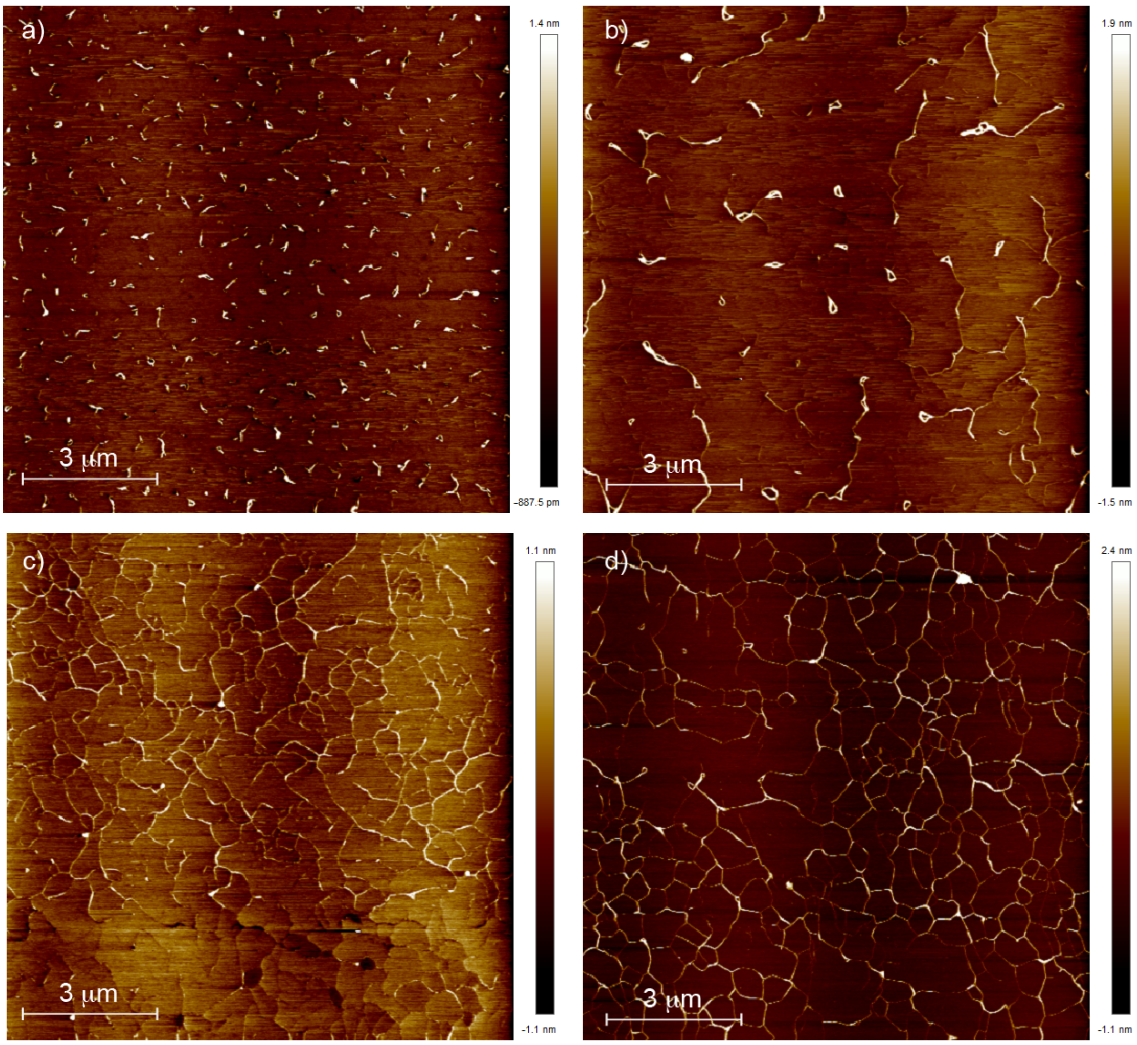

Figure S13. AFM images of a mixture of ***(S)*-1** and ***(R)*-1** at *ee* = 0.4 after 15 min (a); 2 h (b), 4 h (c) and 24 h(d) upon preparing the mixture (MCH, cT = 20 μM; 298 K).

2. Simulations of the MR experiment.

Simulations of the evolution of the equivalent concentrations and the copolymer length of all the monomeric and aggregated species versus the enantiomeric excess have been carried out by the Matlab® script "Example_NatureComm2011" published by Ten Eikelder et al.[S1] This model considers the formation of a chiral copolymer by mixing two enantiomers. The simulated curves correspond to values of c_T = 20 μM and a temperature of 293 K (Figures 3c and 3d in the main text).
These simulations are based on a mass balance model and on the thermodynamic parameters collected in Table S1 and derived by the one-component and two-components EQ models Matlab® scripts described by ten Eikelder et al.[S2] To simplify the name of the involved species, the correspondence between the names is the following:

- free a = ***(S)*-1** monomers;
- free b = ***(R)*-1** monomers;
- A = supramolecular polymer formed by ***(S)*-1**;
- B = supramolecular polymer formed by ***(R)*-1**;
- M and P indicate the handedness of the helical supramolecular polymer. Thus, P^A and P^B indicate the supramolecular polymers of *P*-type handedness formed by ***(S)*-1** and ***(R)*-1**; M^A and M^B indicate the supramolecular polymers of *M*-type handedness formed by ***(S)*-1** and ***(R)*-1**.

This simulation has been performed by considering that the enantiomer in excess is tricarboxamide ***(S)*-1** that upon self-assembly affords *M*-type helical supramolecular polymers. The speciation plot displayed in Figure 3c and Figure S12 shows the negligible presence of free monomers in the mixture and the drop in the equivalent concentration of the *P*-type helical aggregates formed by both ***(S)*-1** and ***(R)*-1**. The simulation predicts, in very good agreement with the experimental evidence, that at *ee* = 0.33 a homochiral coassembly is achieved.

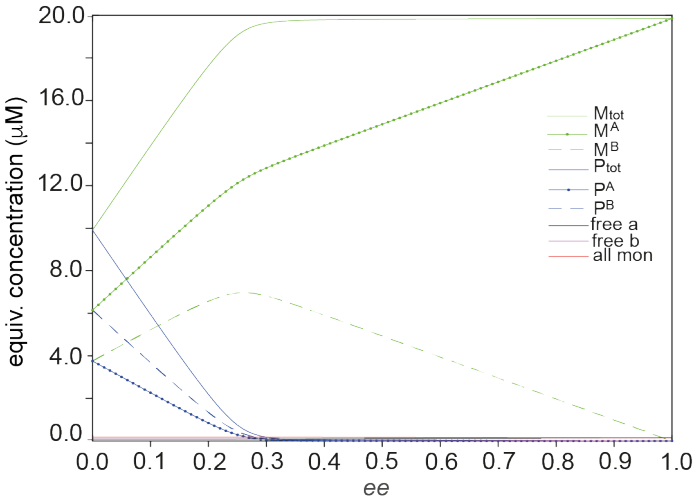

Figure S14. Simulation of the copolymerization of ***(S)*-1** and ***(R)*-1** in the MR experiment (MCH, c_T = 20 μM, 293 K) showing the equivalent concentration of polymers and monomers. Legend: free a = ***(S)*-1** monomers; free b = ***(R)*-1** monomers; A = supramolecular polymer formed by ***(S)*-1** and B = supramolecular polymer formed by ***(R)*-1**; *M* and *P* indicate the handedness of the helical supramolecular polymer.

3. Experimental section

General. All solvents were dried according to standard procedures. Reagents were used as purchased. All air-sensitive reactions were carried out under argon atmosphere. Flash chromatography was performed using silica gel (Merck, Kieselgel 60, 230-240 mesh or Scharlau 60, 230-240 mesh). Analytical thin layer chromatography (TLC) was performed using aluminium-coated Merck Kieselgel 60 F254 plates. NMR spectra were recorded on a Bruker Avance 300 (^{1}H: 300 MHz; ^{13}C: 75 MHz) and on a Bruker Avance 700 (^{1}H: 700 MHz; ^{13}C: 175 MHz) spectrometer using partially deuterated solvents as internal standards. Coupling constants (*J*) are denoted in Hz and chemical shifts (δ) in ppm. Multiplicities are denoted as follows: s = singlet, d = doublet, t = triplet, q = quadruplet, m = multiplet, br = broad. FT-IR spectra in film were recorded on a Bruker Tensor 27 (ATR device) spectrometer. FT- IR spectra in solution were recorded on a JASCO-FT-IR-6800 equipped with a CaF_2 cell with a path length of 0.1 mm. UV-Vis spectra were registered on a Jasco-V630 spectrophotometer equipped with a Peltier thermoelectric temperature controller. The spectra were recorded in the continuous mode between 220 and 500 nm, with a wavelength increment of 1 nm, a response time of 4 s, and a bandwidth of 1 nm, by using a quartz cuvette (Hellma). Thermal experiments were performed at constant heating rates of 1 K min^{-1} from 283 to 363 K in methylcyclohexane. Circular dichroism (CD) measurements were performed on a JASCO-1500 dichrograph equipped with a Peltier thermoelectric temperature controller. The spectra were recorded in the continuous mode between 220 and 500 nm, with a wavelength increment of 0.2 nm, a response time of 1 s, and a bandwidth of 2 nm using a quartz cuvette (Hellma). Matrix Assisted Laser Desorption Ionization (coupled to a Time-Of-Flight analyzer) experiments (MALDI-TOF) were recorded on a Bruker REFLEX spectrometer. AFM measurements were performed under ambient conditions using a MultiMode 8HR SPM from Bruker operating in tapping mode in air. Silicon cantilevers with a resonance frequency of 300 kHz were used. Solutions of compounds ***(S)*-1** and ***(R)*-1** were spin-coated onto mica.

4. Synthetic details and characterization

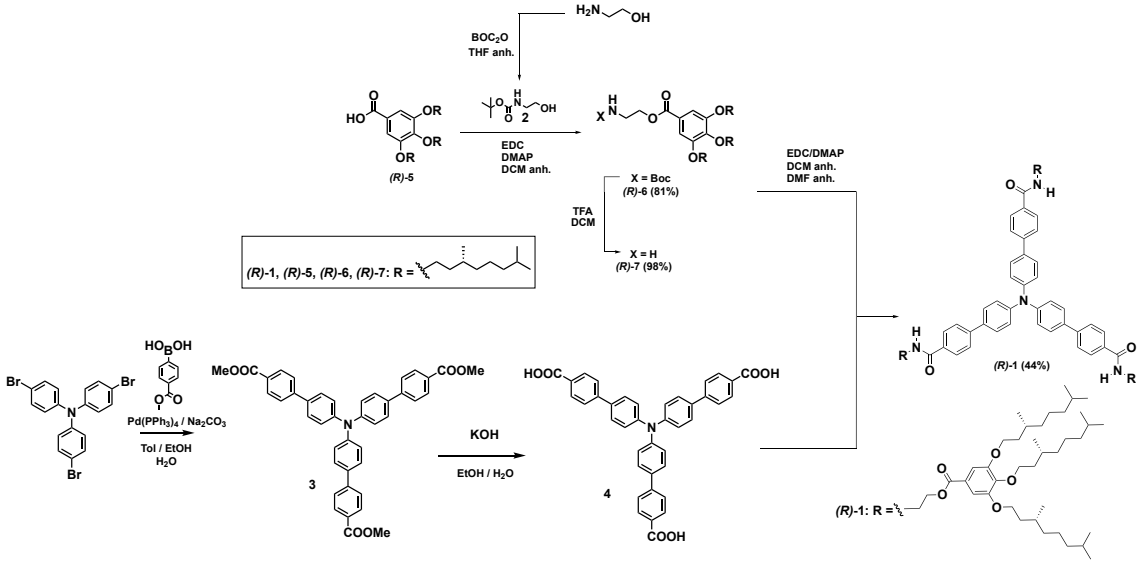

Compound **2, 3**[S3] and **(*R*)-5**[S4] were prepared according to previously reported synthetic procedures and showed identical spectroscopic properties to those reported therein.

2-((*Tert*-butoxycarbonyl)amino)ethyl 3,4,5-tris(((*R*)-3,7-dimethyloctyl)oxy)-benzoate (*R*-6)

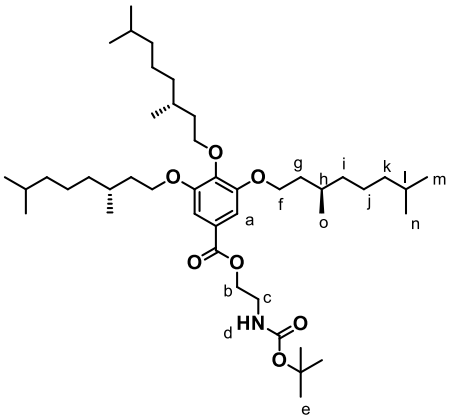

To a stirred solution of ***(R)*-5** (1.0 g, 1.52 mmol) in 15 mL of anhydrous dichloromethane, 1-ethyl-3-(3-dimethylaminopropyl)carbodiimide hydrochloride (322 mg, 1.68 mmol) and 4-dimethylaminopyridine (205 mg, 1.68 mmol) were added portionwise at 0°C and under argon atmosphere. After fifteen minutes, *tert*-butyl (2-hydroxyethyl)carbamate (270 mg, 1.68 mmol) was added and the reaction mixture was stirred overnight at room temperature. The resulting crude was washed with HCl (1 M) and an aqueous NaCl solution and dried over $MgSO_4$. After filtration and removal of the solvent, the residue was subjected to a silica gel chromatography column (hexane 9:1 ethyl acetate as eluent) affording

compound **(*R*)-6** as yellow oil in 81% yield (800 mg, 0.97 mmol). ^{1}H NMR (300 MHz, $CDCl_3$ (δ / ppm): 7.26 (s, 2H, H_a), 4.83 (br, 1H, H_d), 4.36 (t, 2H, H_b, J = 5.28), 4.04 (m, 6H, H_f), 3.53 (m, 2H, H_c), 1.58 (m, 30H, $H_{g,h,i,j,k,l}$), 0.95 (d, 9H, H_e), 0.93 (d, 9H, H_o, J = 2.07), 0.87 (d, 18H, $H_{n,m}$, J = 2.52). ^{13}C NMR (75 MHz, $CDCl_3$) (δ / ppm): 169.8, 163.3, 155.7, 152.8, 142.5, 124.6, 108.3, 79.7, 71.6, 67.5, 64.2, 61.1, 39.9, 39.8, 39.3, 39.2, 37.4, 37.3, 36.3, 29.7, 29.6, 29.4, 28.3, 27.9, 24.6, 22.6, 22.5, 19.5. FTIR (v /cm^{-1}): 764, 866, 1042, 1110, 1166, 1209, 1331, 1383, 1462, 1500, 1586, 1716, 2925, 3373. MALDI-MS: $C_{44}H_{79}NO_7$ $[M]^+$ calcd. 733.585; found, 733.508.

2-Aminoethyl 3,4,5-tris(((*R*)-3,7-dimethyloctyl)oxy)benzoate (*R*-7)

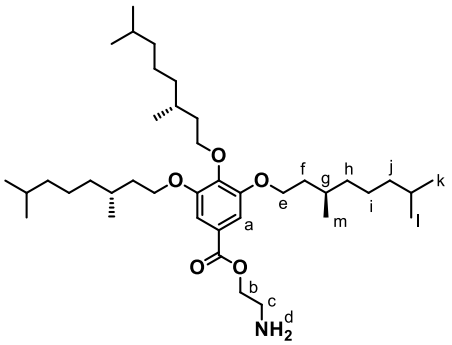

To a stirred solution of ***(R)*-6** (600 mg, 0.73 mmol) in 15 mL of anhydrous dichloromethane was added trifluoroacetic acid (1.46 mL) and the reaction mixture was stirred an hour at room temperature. The resulting crude was washed with H_2O and dried over $MgSO_4$. After filtration and removal of the solvent, the residue was affording as a pale yellow oil in 98% yield (600 mg, 0.83 mmol).^{1}H NMR (300 MHz, $CDCl_3$ (δ / ppm): 7.22 (s, 2H, H_a), 4.58 (br, 2H, H_d), 4.02 (m, 6H, H_e), 3.43 (s_{br}, 4H, $H_{b,c}$), 1.19 (m, 30H, $H_{f,g,h,i,j}$), 0.92 (d, 9H, H_m, J = 3.17), 0.85 (d, 18H, $H_{k,l}$, J = 6.62). ^{13}C NMR (75 MHz, $CDCl_3$) (δ / ppm): 167.40, 152.92, 122.87, 108.35, 101.90, 76.59, 69.30, 67.55, 61.46, 39.26, 37.49, 37.38, 36.30, 31.94, 30.31, 29.72, 29.66, 29.39, 29.34, 29.31, 27.9, 26.1, 24.7, 22.7, 22.6, 19.4, 14.1. FTIR (v /cm^{-1}): 762, 1008, 1116, 1207, 1334, 1379, 1432, 1464, 1587, 1688, 1784, 2853, 2922, 3188. MALDI-MS: $C_{39}H_{71}NO_5$ $[M]^+$ calcd. 633.533; found, 633.410.

Compound (*R*)-1

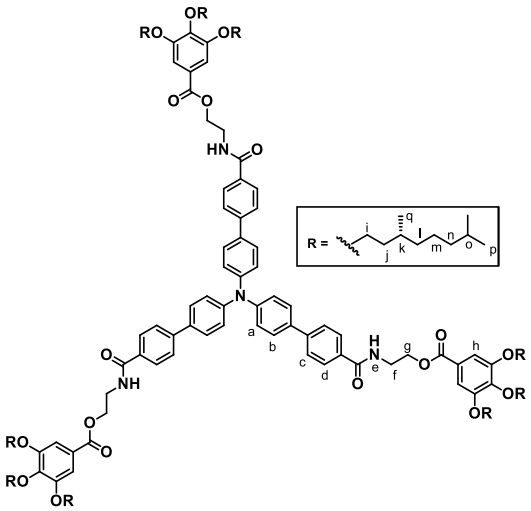

Tricarboxylic acid **4** (50 mg, 0.053 mmol) was dissolved in dichloromethane (5 mL) and dimethylformamide (1 mL). To this solution, 1-ethyl-3-(3-dimethylaminopropyl)-carbodiimide hydrochloride (71 mg, 0.37 mmol) and 4-dimethylaminopyridine (45 mg, 0.37 mmol) were added portionwise at 0ºC and under argon atmosphere. After fifteen minutes, compound ***(R)-7*** (270 mg, 0.37 mmol) was added and the reaction mixture was stirred overnight at room temperature. The resulting crude was washed with HCl (1 M) and an aqueous NaCl solution and dried over $MgSO_4$. After filtration and removal of the solvent, the residue was subjected to a silica gel chromatography column (dichloromethane 10:0.2 methanol as eluent), affording compound ***(R)*-1** as a pale yellow solid in 44% yield (87 mg, 0.035 mmol). ^{1}H NMR (700 MHz, $CDCl_3$ (δ / ppm): 7.82 (d, 6H, H_d, J = 9.20), 7.60 (d, 6H, H_c, J = 8.76), 7.51 (d, 6H, H_b, J = 8.32), 7.22 (d, 6H, H_a, J = 3.07), 7.19 (s, 6H, H_h), 6.70 (t, 3H, H_e, J = 5.85), 4.53 (t, 6H, H_g, J = 6.75), 4.01 (m, 18H, H_i), 3.86 (m, 6H, H_f), 1.38 (m, 90H, $H_{j,k,l,m,n,o}$), 0.89 (t, 27H, H_q, J = 6.17), 0.82 (d, 54H, $H_{p,r}$, J = 6.60) . ^{13}C NMR (75 MHz, $CDCl_3$) (δ / ppm): 165.30, 165.06, 150.91, 145.18, 141.58, 140.75, 132.54, 130.50, 126.08, 125.56, 124.68, 122.53, 122.17, 106.15, 69.76, 65.53, 61.82, 37.92, 37.34, 37.25, 35.47, 35.35, 35.32, 34.32, 27.81, 27.62, 25.97, 22.73, 22.70, 20.70, 20.60, 17.57. FTIR (v /cm^{-1}): 767, 827, 1114, 1210, 1333, 1381, 1431, 1464, 1494, 1541, 1636, 1717, 2855, 2925, 2954, 3352. MALDI-MS: $C_{156}H_{234}N_4O_{18}$ $[M]^+$ calcd. 2451.7518; found, 2451.7464.

5. Collection of spectra

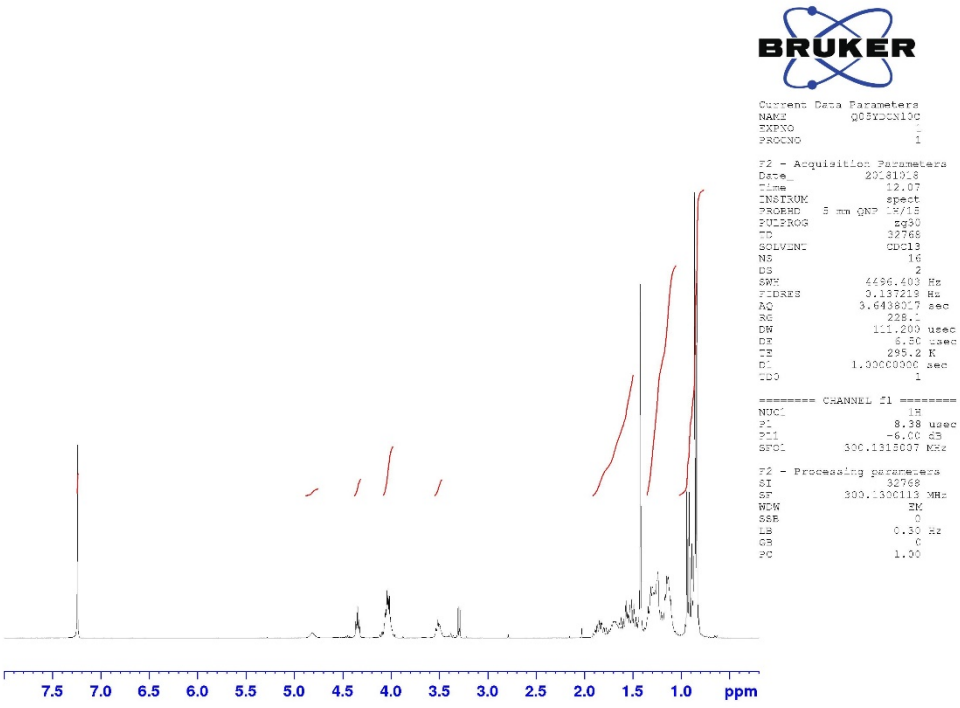

^{1}H NMR spectrum of compound ***(R)*-6** (300 MHz, $CDCl_3$, 298 K).

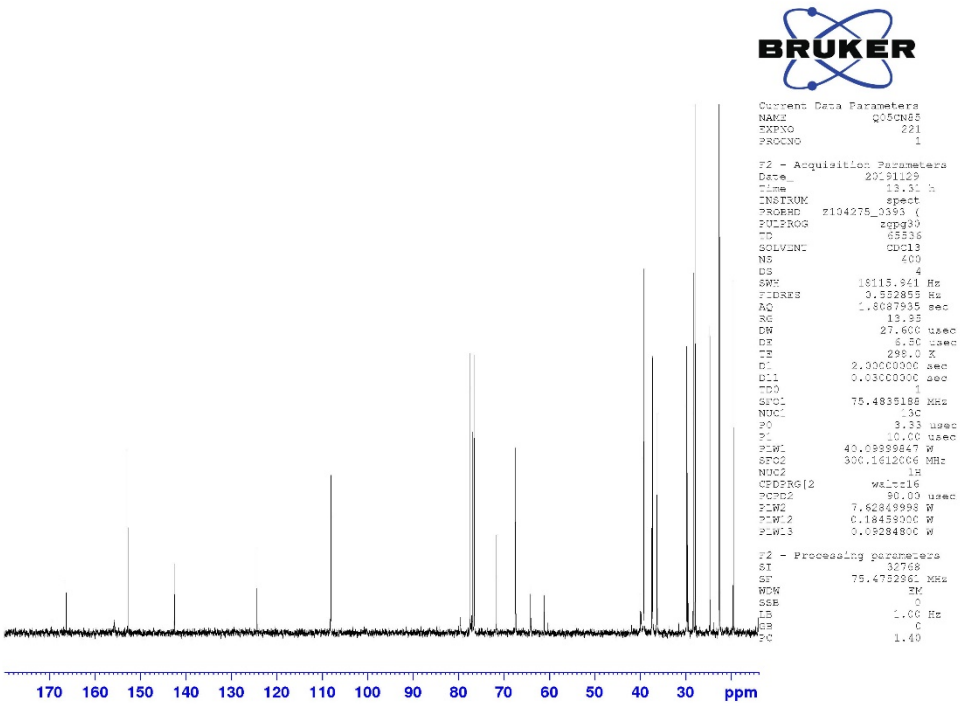

^{13}C NMR spectrum of compound ***(R)*-6** (75 MHz, $CDCl_3$, 298 K).

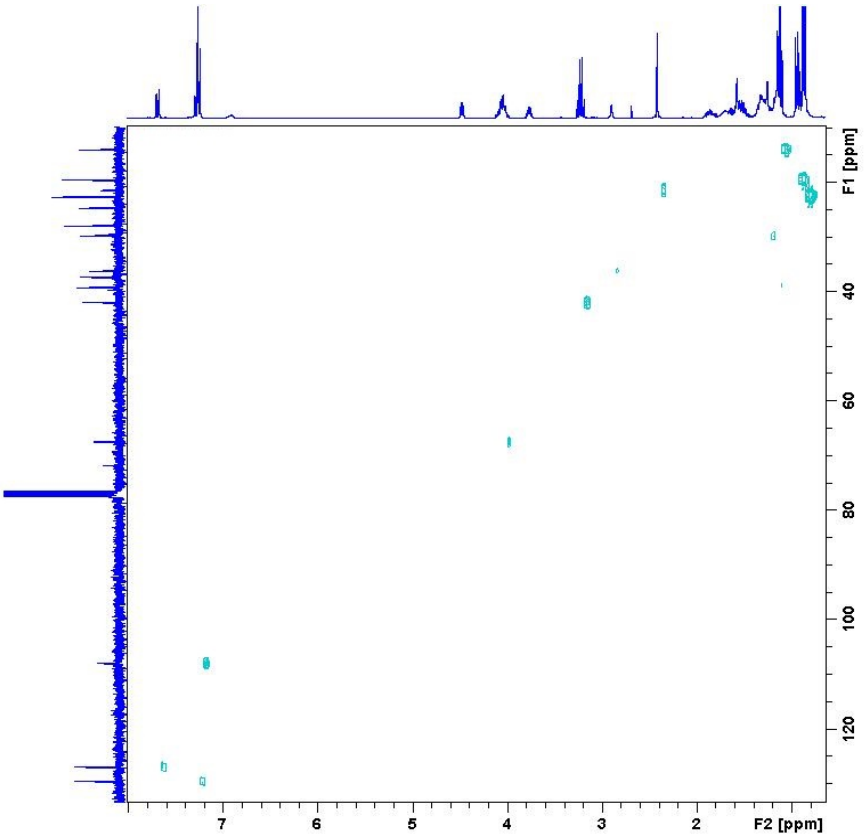

^{1}H, ^{13}C-HMQC spectrum ($CDCl_3$, 298 K) of compound ***(R)*-6**.

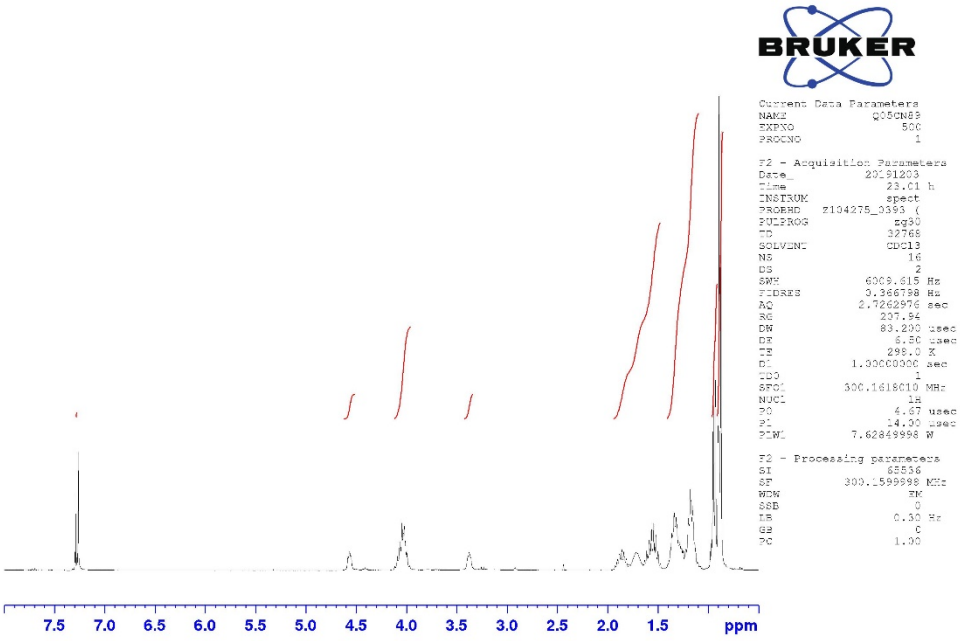

^{1}H NMR spectrum of compound ***(R)*-7** (300 MHz, $CDCl_3$, 298 K).

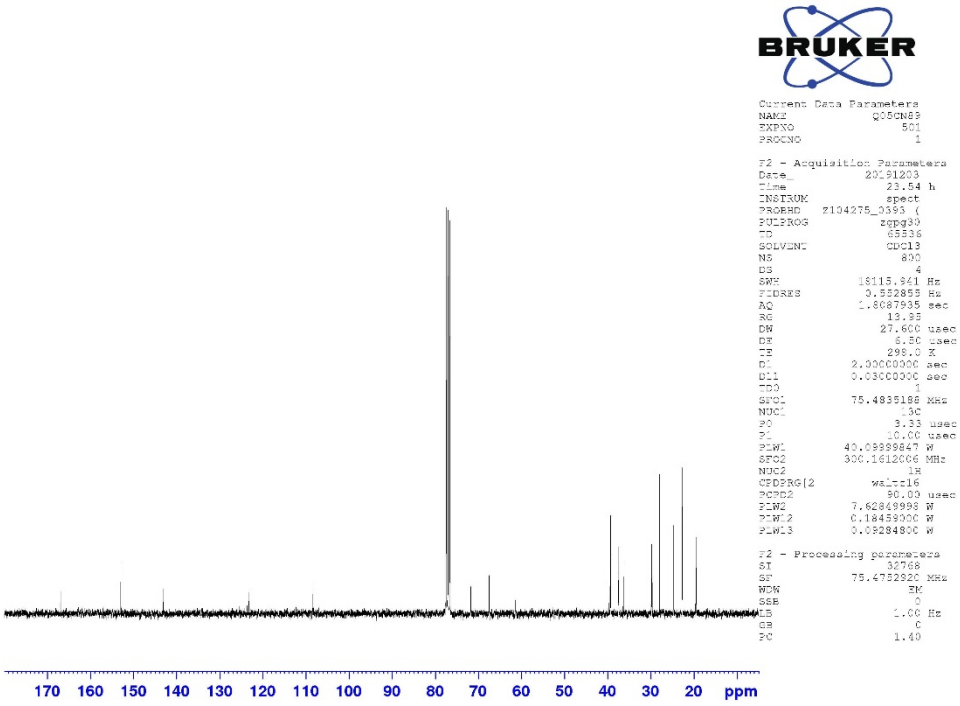

^{13}C NMR spectrum of compound ***(R)-7*** (75 MHz, $CDCl_3$, 298 K).

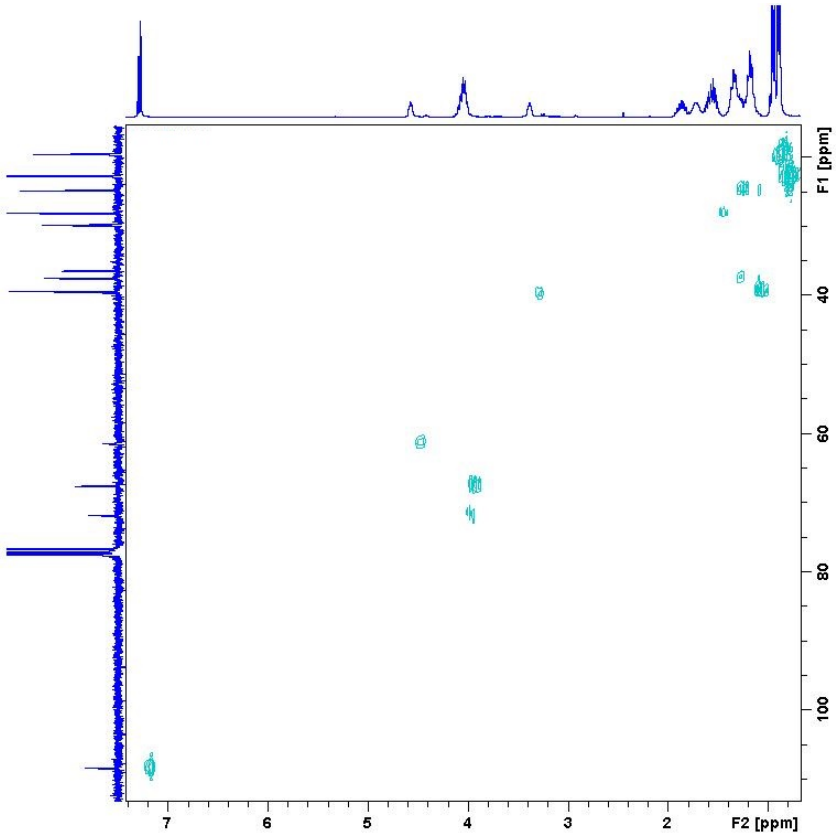

^{1}H, ^{13}C-HMQC spectrum ($CDCl_3$, 298 K) of compound ***(R)-7***.

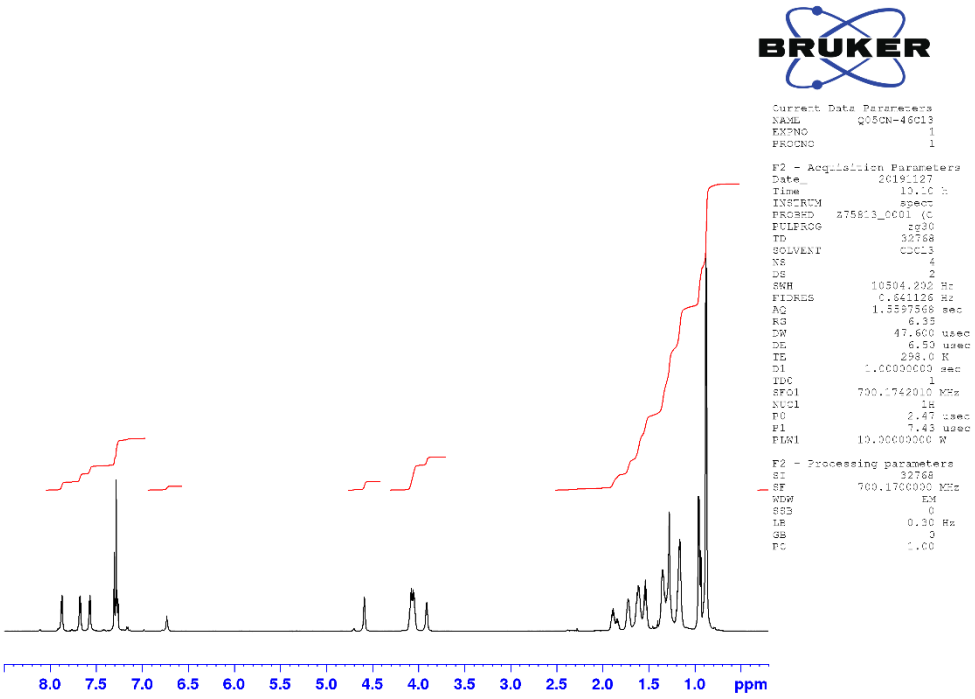

^{1}H NMR spectrum of compound ***(R)*-1** (700 MHz, $CDCl_3$, 298 K).

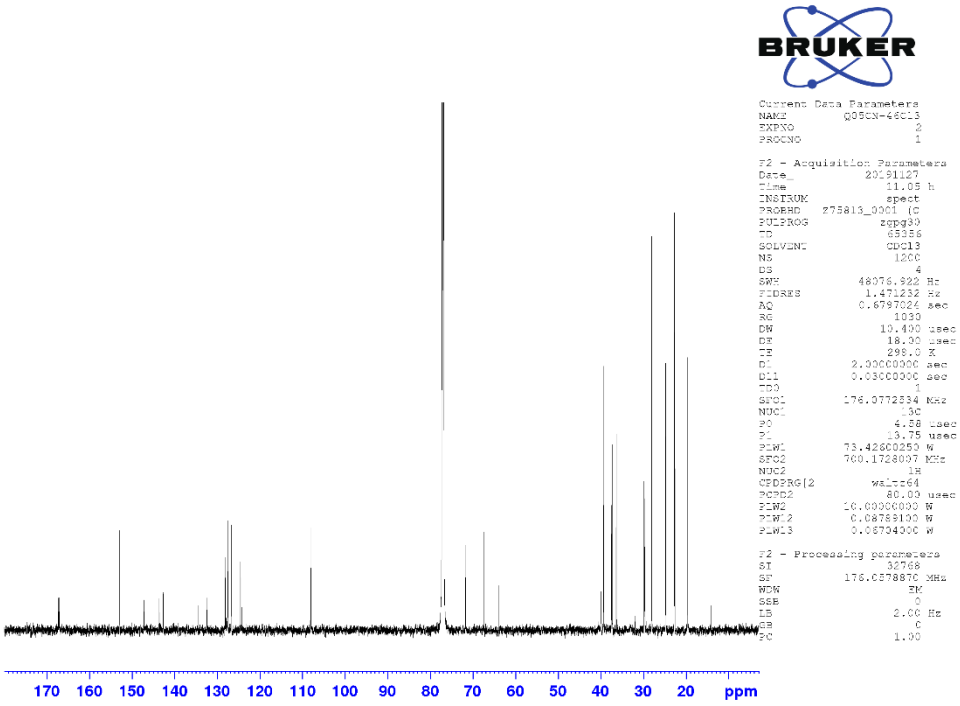

^{13}C NMR spectrum of compound ***(R)*-1** (175 MHz, $CDCl_3$, 298 K).

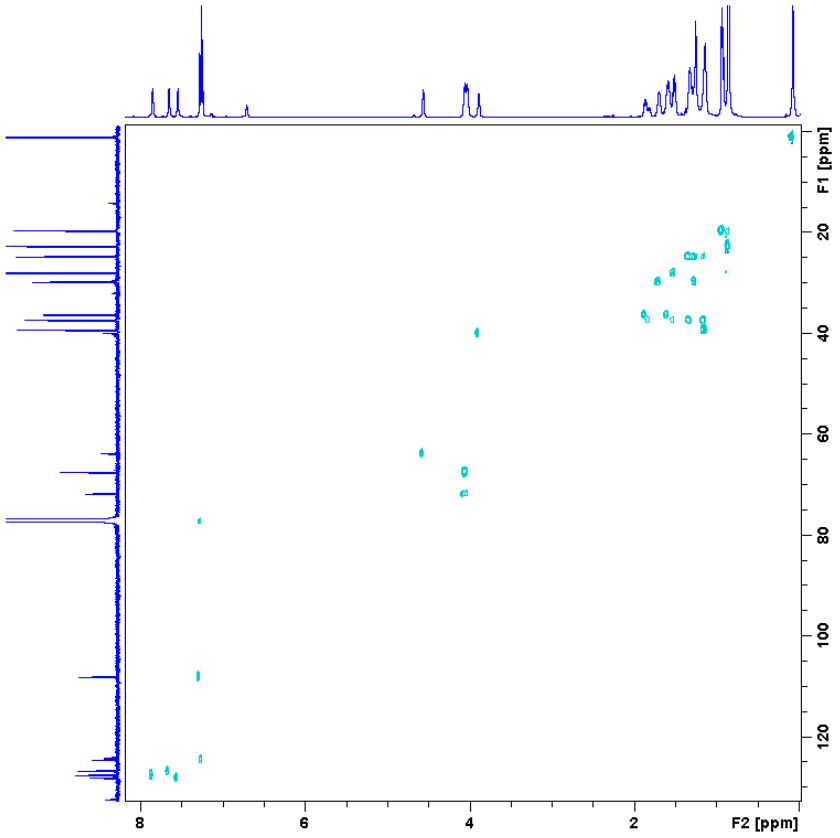

^{1}H, ^{13}C-HMQC spectrum ($CDCl_3$, 298 K) of compound ***(R)*-1**.

6. References

S1. H. M. M. ten Eikelder, B. Adelizzi, A. R. A. Palmans and A. J. Markvoort, *J. Phys. Chem. B* 2019, **123**, 6627.

S2. H. M. M. ten Eikelder, A. J. Markvoort, T. F. A. de Greef and P. A. J. Hilbers, *J. Phys. Chem. B* 2012, **116**, 5291.

S3. Y. Zhang, Y.-Q. Feng, J.-H. Wang, G. Han, M.-Y. Li, Y. Xia and Z.-D. Feng, *RSC Adv.* 2017, **7**, 35672.

S4. E. E. Greciano, B. Matarranz and L. Sánchez, *Angew. Chem Int. Ed.* 2018, **57**, 4697.